



**HAL**  
open science

# A viscoelastic–viscoplastic model with hygromechanical coupling for flax fibre reinforced polymer composites

Marwa Abida, Florian Gehring, Jamel Mars, Alexandre Vivet, Fakhreddine Dammak, Mohamed Haddar

## ► To cite this version:

Marwa Abida, Florian Gehring, Jamel Mars, Alexandre Vivet, Fakhreddine Dammak, et al.. A viscoelastic–viscoplastic model with hygromechanical coupling for flax fibre reinforced polymer composites. Composites Science and Technology, 2020, 189, pp.108018. 10.1016/J.COMPSCITECH.2020.108018 . hal-03164294

**HAL Id: hal-03164294**

**<https://hal.science/hal-03164294>**

Submitted on 21 Jul 2022

**HAL** is a multi-disciplinary open access archive for the deposit and dissemination of scientific research documents, whether they are published or not. The documents may come from teaching and research institutions in France or abroad, or from public or private research centers.

L'archive ouverte pluridisciplinaire **HAL**, est destinée au dépôt et à la diffusion de documents scientifiques de niveau recherche, publiés ou non, émanant des établissements d'enseignement et de recherche français ou étrangers, des laboratoires publics ou privés.



Distributed under a Creative Commons Attribution - NonCommercial 4.0 International License

# A viscoelastic-viscoplastic model with hygromechanical coupling for flax fibre reinforced polymer composites

Marwa ABIDA<sup>a,\*</sup>, Florian GEHRING<sup>a</sup>, Jamel MARS<sup>c</sup>, Alexandre VIVET<sup>a</sup>,  
Fakhreddine DAMMAK<sup>c</sup>, Mohamed HADDAR<sup>b</sup>

<sup>a</sup>*Normandie Univ, ENSICAEN, UNICAEN, CEA, CNRS, CIMAP, 14000 Caen, France*

<sup>b</sup>*LA2MP, National Engineering School of Sfax, B.P 1173-3038, Sfax, University of Sfax, Tunisia*

<sup>c</sup>*LASEM, National Engineering School of Sfax, B.P W3038, Sfax, University of Sfax, Tunisia*

---

## Abstract

Based on experimental investigations on the influence of water content on time-dependent behaviour of flax reinforced epoxy composites, this paper proposes to model the viscoelastic-viscoplastic behaviour with hygromechanical coupling. From a rheological point of view, the proposed model is a combination of a linear spring (elasticity), a Kelvin-Voigt model (viscoelasticity) and a viscoplastic model described by kinematic hardening in which the evolution of the internal variable is collinear with the plastic deformation. The hygromechanical coupling is obtained via the dependence on water content of all the model parameters according to a power law. The developed model shows a good correlation between experimental data (tensile, creep and relaxation) and numerical predictions of the mechanical behaviour for low water contents (below 4.90%). However, the model shows its limits for high water contents ( $w_c \geq 4.90\%$ ) and high loadings. **Indeed, tensile tests have revealed the emergence of a stiffening phenomenon for high loadings according to water content. This phenomenon was not taken into account in the proposed model which could explain its limitations.** This assumption is confirmed by comparing the evolution of experimental yield stress with the model prediction.

---

\*Corresponding author

Email address: [marwa.abida@unicaen.fr](mailto:marwa.abida@unicaen.fr) (Marwa ABIDA)

*Keywords:* constitutive modelling, flax fibre, composite, time-dependent behaviour, hygromechanical coupling

---

## 1. Introduction

Contrary to synthetic fibre reinforced composites (glass, carbon, etc.), composites reinforced with plant fibres exhibit a highly non-linear behaviour. Indeed, the monotonic tensile curves are characterized by the presence of an apparent yield point. This phenomenon has been observed on plant fibre reinforced composites in general ([1, 2]) and on flax fibre reinforced composites in particular ([3, 4, 5, 6, 7]), regardless the reinforcement architecture (unidirectional reinforcement ([3, 1]), random mat reinforcements ([3, 8])). In some favorable experimental conditions, an inflection point is observed in the tensile curve leading to an apparent rigidification of plant fibre reinforced composites (PFRC), even under infinitesimal strains. All experimental investigations show that PFRC behaviour needs to be considered as viscoelastic and viscoplastic.

In addition, the mechanical behaviour is greatly affected by the external conditions (UV, humidity, temperature...). In literature, some studies on the influence of water ageing on the mechanical properties of PFRC can be found. These studies generally point out that PFRC show a decrease in Young's modulus and in the ultimate tensile strength, and an increase in elongation at break when placed in humid atmosphere or immersed in water for instance. These results have been observed on hemp ([9, 10]), flax ([11, 12, 13, 14]), kenaf ([15]) or cellulosebased reinforcements ([16]). Contrary to all the expectations following the work of Mannan and Robbany [17], a study conducted by Placet et al. [18] shows an increase of hemp fibre apparent modulus with the increase of relative humidity up to a critical point. The authors assume that this change could be due to the modification of physical properties of hemp fibre. More recently, Abida et al.[19] show that the evolution of mechanical properties (rigidity, elongation) of flax reinforcement according to water content is non-linear. The study of hygromechanical coupling in PFRC global behaviour is therefore a major is-

28 sue.

29 The different proposed models of PFRC behaviour can be classified into sev-  
30 eral groups. The first is interested in phenomenological modelling of viscoelastic  
31 or even viscoelastoplastic behaviour ([20, 21, 6, 22, 23, 2, 24]). Marklund et al.  
32 [20] develop a viscoelastic viscoplastic model of hemp / lignin composites with  
33 consideration of damage. Schapery's theory [25] coupled with the Boltzmann's  
34 superposition principle is used by Kontou et al. [21] to model the non-linear  
35 viscoelasticity and non-linear viscoplasticity of composites. Poilane et al. [6]  
36 and Richard et al. [24] propose a phenomenological viscoelastoplastic model to  
37 study the non-linear effects of viscoelastic and viscoplastic phenomena of plant  
38 fibre composites. More recently, Pupure et al. [26] proposed a macro-scale  
39 viscoelastic-viscoplastic model for regenerated cellulose fiber (RCF) composites.  
40 The viscoelasticity is described by Schapery's models [25] and the viscoplastic-  
41 ity is described by Zapas' model[27]. These models are often limited to uniaxial  
42 loading. Abida et al. [28] propose an anisotropic viscoelastic-viscoplastic model.  
43 The orthotropic viscoplasticity is described by the Hill criterion and a modified  
44 Johnson-Cook type hardening. The second group is interested in hygromechan-  
45 ical coupling. This work is often limited to the elastic domain and is limited  
46 to the determination of the coefficient of hygro-expansion and its influence on  
47 the residual stresses ([29, 30, 31]). Le Duigou et al. [29] evaluate the resid-  
48 ual stresses using thermal and the hygroscopic swelling coefficient in an elastic  
49 model. This study highlights the importance of the interfacial stresses resulting  
50 from the differential fibre and matrix swellings. Chilali et al. [31] have also  
51 demonstrated by a finite element method the high concentration of stress at the  
52 fibre / matrix interface generated by the differential swellings. However, few  
53 studies present a hygromechanical coupling models considering the composites  
54 as viscoelastic-viscoplastic materials.

55 This paper is devoted to present a first approach to model viscoelastic-  
56 viscoplastic behaviour with hygromechanical coupling. The paper firstly pro-  
57 ceeds with a description of the materials and the method used to obtain com-  
58 posite samples with different water contents (section 2). Then, an overview of

59 the mechanical behaviour of flax reinforced epoxy composite is proposed in sec-  
60 tion 3. The paper focus on the influence of water content on the time-dependent  
61 behaviour of flax reinforced epoxy composites. The hypotheses, the constitutive  
62 equations and the identification strategy of the model will then be presented and  
63 described in section 4. The performance of the model is discussed in last section  
64 (section 5).

## 65 2. Materials and experimental procedures

### 66 2.1. Materials and specimen manufacturing

67 The reinforcement is a quasi-unidirectional flax yarn fabric manufactured by  
68 LINEO NV Company commercially known as FUD180. The basic weight of the  
69 fabric is  $180 \text{ g/m}^2$ . This woven fabric contains yarns in the weft direction in  
70 order to facilitate its handling. Its balancing coefficient is 0.93. This coefficient  
71 corresponds to the ratio of the volume of warp yarns and the total volume of  
72 yarns (warp and weft). A ratio of 1 weft yarn for 15 warp yarns is found.

73 The matrix is an epoxy system consisting of a combination of a resin (LY  
74 1546) and a hardener (Aradur 3787) supplied by HUNTSMAN Corporation.

75 Flax / epoxy composite laminates are manufactured by contact moulding  
76 in closed mould using the same warp yarns orientation for each ply. In order  
77 to manufacture unidirectional composite laminates, the flax reinforcements are  
78 firstly dried for one hour at  $110 \text{ }^\circ \text{C}$  in order to eliminate water molecules. Each  
79 reinforcement ply is then manually impregnated and stacked. The laminate is  
80 then kept under compression at ambient temperature for two hours before curing  
81 at  $100 \text{ }^\circ \text{C}$  for two hours. The tensile specimens,  $200 \text{ mm} \times 20 \text{ mm} \times 2 \text{ mm}$ , are  
82 cut using a laser machine Trotec speedy 400. Sample-cutting parameters (speed  
83 and power) have been adjusted and optimised to avoid edges' burning. A glass  
84 transition temperature  $T_g$  of  $110 \pm 2^\circ \text{C}$  for composite samples was measured in  
85 twisting/relaxation loading mode using Kinetech® (DMA-like mode).

86 *2.2. Conditioning and monitoring protocol*

87 The conditioning protocol was previously used and described in Abida et al.  
88 [19]. The main steps are reminded in the following. All composite specimens  
89 are dried at 103 ° C for 24 h to ensure total removal of water (no significant  
90 mass change is found after 24 h of drying). Epoxy is assumed insensitive to  
91 water ([5]) and all water molecules are supposed to be evaporated during dry-  
92 ing. Once dried, they are weighed and conditioned in an **climatic** chamber at  
93 constant relative humidity using saturated saline solutions until stabilization of  
94 the water uptake. Specimens mass monitoring is performed periodically in order  
95 to determine their absorbed water content over time. Flax / epoxy composite  
96 specimens weigh around 10 g, and they are weighed on a  $10^{-4}$  g precision **scale**  
97 (Mettler Toledo). Therefore, the moisture regain is considered as water content  
98 ( $w_c$ ) in flax / epoxy composite and evaluated using equation (eq. 1).

$$w_c (\%) = \frac{m(t) - m_{dried}}{m_{dried}} \times 100 \quad (1)$$

99  
100 where  $m(t)$  is the mass over time and  $m_{dried}$  the mass measured after drying.

101 The table (tab. 1) provides the conditioning atmosphere and the correspond-  
102 ing water content of composite laminates at saturation when  $m(t)$  reached the  
103 saturated mass  $m_{saturated}$ .

104 *2.3. Experimental tests*

105 The time-dependent behaviour in principal direction (**warp yarns direction**)  
106 of flax / epoxy composite are investigated by **performing tensile, creep and**  
107 **relaxation tests** using an Instron hydraulic machine equipped with a 100 *kN*  
108 cell load. An extensometer with a gauge length of 50 *mm* is used to measure  
109 the longitudinal strain. **The tensile and relaxation tests were strain controlled**  
110 **and the creep tests were load controlled. The tensile behaviour were obtained**  
111 **at conventional strain rate of  $10^{-4} s^{-1}$ .** The creep tests consists in loading to  
112 a chosen stress, **then holding at constant stress for 15 min (creep)**, unloading

Table 1: water content of flax/epoxy composite according conditioning

Aqueous saturated saline solution or atmosphere	RH at 20° C ( %)	Flax/epoxy composite water content ( %)
Dried	-	0*
Potassium hydroxide ( <i>KOH</i> )	8	0.63 ± 0.03
Potassium Carbonate ( <i>K<sub>2</sub>CO<sub>3</sub></i> )	45	2.40 ± 0.10
Sodium Chloride ( <i>NaCl</i> )	75	4.90 ± 0.20
Potassium Sulphate ( <i>K<sub>2</sub>SO<sub>4</sub></i> )	97	10.50 ± 0.01
Immersed	-	14.40 ± 0.10

\*supposed to be 0 %

113 to zero stress followed by a **strain recovery for a time of 15 min**. The total  
114 time of tests should be less than 30 min to ensure that water content remains  
115 constant over test time. Moreover a recovery time of 3 hours after a creep of  
116 15 min was tested. Results showed a less than 1 % difference between both  
117 viscoplastic strains and thus allowed to limit the recovery time to 15 min. Two  
118 stress levels are tested for each water content. The first stress level is set at 75 %  
119 of the apparent ultimate stress. The apparent ultimate stress were obtained by  
120 previous monotonic tensile tests. The second level is lower than the apparent  
121 initial yield stress. The stress rate has been set at  $6 \text{ MPa} \cdot \text{s}^{-1}$  in order to limit  
122 the loading and unloading times. **In relaxation tests, the specimen is loaded to**  
123 **certain strain level and then the total strain is kept constant for 15 min allowing**  
124 **for stress relaxation. Then, the specimen is unloaded to a lower strain (partial**  
125 **unloading) and the total strain is kept constant for 15 min. After unloading,**  
126 **the sample is still in tension to avoid buckling. Both of strain levels were chosen**  
127 **in accordance with the tensile behaviour. In all figures dealing with relaxation**  
128 **tests  $\epsilon_l$  refers to the initial strain level and  $\epsilon_u$  refers to the strain after partial**  
129 **unloading. The loading and the unloading rates were set to  $10^{-2} \text{ s}^{-1}$ . In**  
130 **creep and relaxation tests, the holding times were chosen in accordance with**  
131 **diffusion kinetics to limit the variation of water content during tests. The entire**

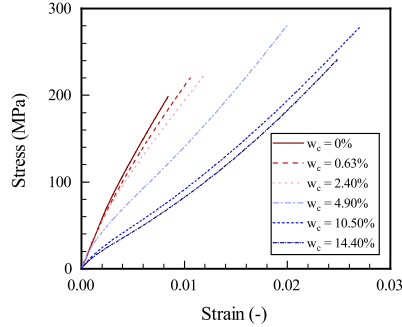


Figure 1: tensile behaviour of flax/epoxy composite according to water content

132 database is therefore composed of 2 creep tests and 2 relaxation tests for each  
 133 water content, which means 24 tests.

### 134 3. Experimental investigations

135 PFRCs often present non-linear mechanical behaviour. This non-linearity is  
 136 observed for the studied flax / epoxy composite whatever the water content. It  
 137 is worth to note that water content has a strong influence on the mechanical  
 138 behaviour of flax / epoxy composite (figure 1).

139 At low water contents (below 4.90 %), the typical tensile curves of PFRC are  
 140 observed. Indeed, this phenomenon could be explained by structural changes  
 141 within the fibre ([32] among others) such as the reorientation of cellulose mi-  
 142 crofibrils in wall irregularities (kink band areas), the spiral spring-like exten-  
 143 sion of cellulose microfibrils, and the shear-stress-induced crystallization of the  
 144 amorphous cellulose of the flax fibres. The Young modulus for dried flax/epoxy  
 145 composite specimens is around 30 GPa and it sharply drops of 60 %, that is to  
 146 say 12 GPa when composite water content increases to 14.40 %.

147 The time-dependent behaviour of flax / epoxy composites with respect to  
 148 water content is investigated (fig. 2). The creep tests are conducted at two  
 149 stress levels: one below the apparent yield point (fig. 2a) and the other at 75 %  
 150 of the ultimate stress (fig. 2b). As pointed out in the figure (fig. 2a), the

151 delayed strain (or creep strain) after a creep stress below the apparent yield  
 152 point is totally recovered after 15 *min* of load removal. The behaviour of flax /  
 153 epoxy composites could then be considered as viscoelastic. Nevertheless, creep  
 154 tests conducted at a stress level close to ultimate stress reveal that the delayed  
 155 strain is partially recovered after load removal ; an irreversible strain is clearly  
 156 noticeable in figure (fig. 2b). In this case, the behaviour is considered to be  
 157 viscoplastic. These tendencies are observed whatever the water content.

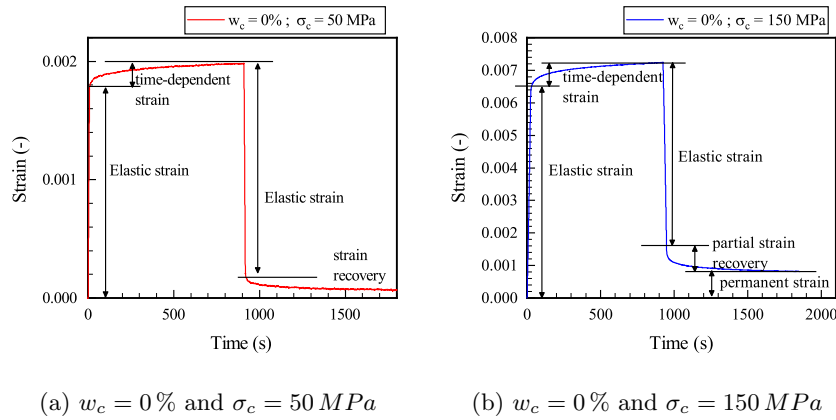


Figure 2: time-dependent behaviour of flax/epoxy composite

158 The experimental investigations point out that flax / epoxy composite be-  
 159 haviour should be considered as viscoelastic-viscoplastic. As water content  
 160 strongly affects the behaviour of studied composites, a viscoelastic-viscoplastic  
 161 model with hygromechanical coupling is proposed in next section.

## 162 4. Constitutive modelling and identification scheme

### 163 4.1. Constitutive modelling

164 As mentioned in the previous section, a viscoelastic-viscoplastic model with  
 165 hygromechanical coupling is developed to predict the mechanical behaviour of  
 166 quasi-unidirectional flax / epoxy composites. The total strain is partitioned  
 167 in an elastic contribution  $\varepsilon_e$  (reversible and instantaneous), a viscoelastic part  
 168  $\varepsilon_{ve}$  (reversible strain and non-instantaneous) and viscoplastic contribution  $\varepsilon_{vp}$

169 (irreversible and non-instantaneous) according to the equation (eq. 2). The vis-  
 170 coelastic and viscoplastic contributions are referred to as inelastic contributions  
 171 in the following.

$$\varepsilon = \varepsilon_e + \varepsilon_{ve} + \varepsilon_{vp} \quad (2)$$

172 In the context of thermodynamics with internal variables ([33]), the stan-  
 173 dardised framework ([34]) assumes that the mechanical behaviour is defined by  
 174 two potentials. A free energy density  $\psi$  is required to define state laws, ex-  
 175 pressed classically by equations (eq. 3 and 4), and by a dissipation potential  $\Omega$   
 176 to determine the evolution of internal variables and therefore the flow direction  
 177 (eq. 5 and 6).

$$\sigma = \rho \cdot \frac{\partial \psi}{\partial \varepsilon_e} \quad (3)$$

$$X_i = \rho \cdot \frac{\partial \psi}{\partial \alpha_i} \quad (4)$$

$$\varepsilon_{ve} + \varepsilon_{vp} = \frac{\partial \Omega}{\partial \sigma} \quad (5)$$

$$\dot{\alpha}_i = - \frac{\partial \Omega}{\partial X_i} \quad (6)$$

178  
 179 where  $\sigma$  is the Cauchy stress,  $\rho$  is the mass density,  $\alpha_i$  are the selected internal  
 180 variables and  $X_i$  the associated variables.

181 According to this approach, it is assumed that in a homogeneous continuous  
 182 medium equivalent to the real material, the microscopic physical phenomena are  
 183 represented by means of macroscopic internal variables. **The model performance**  
 184 **depends on the choice of potentials. In the chosen formalism, the selected**  
 185 **dissipation phenomena are the plasticity and the associated viscosity and the**  
 186 **viscoelasticity. Therefore, two viscosity coefficients drive these phenomena:  $\eta$**   
 187 **in the elastic domain and  $K$  in the plastic domain.** Based on experimental

188 results, it is assumed that elastic and inelastic behaviours are uncoupled and  
 189 that all parameters are depending on water content. In accordance with the  
 190 isothermal loading assumption, the thermal dissipation is not taken into account  
 191 in the modelling. Hence, the two potentials can be proposed as in the following  
 192 equations (eq. 7 and 8).

$$\psi(\varepsilon_e, \alpha_i, w_c) = \frac{1}{2\rho} \cdot E(w_c) \cdot \varepsilon_e^2 + \frac{1}{2\rho} \cdot \sum_{i=1}^2 C_i(w_c) \alpha_i^2 \quad (7)$$

$$\Omega(\sigma, X_i, w_c) = \Omega_{ve} + \Omega_{vp} = \frac{1}{2\eta(w_c)} (\sigma - X_1)^2 + \frac{1}{2K(w_c)} \langle f \rangle^2 \quad (8)$$

$$f = |\sigma - X_2| - \sigma_y(w_c) \quad (9)$$

193  
 194 where  $w_c$  is water content,  $E(w_c)$  the Young's modulus,  $\sigma_y(w_c)$  the initial yield  
 195 stress,  $\eta(w_c)$  and  $K(w_c)$  are the viscosity coefficients in the elastic and plastic  
 196 domain respectively,  $C_1(w_c)$  is the viscoelastic stiffness and  $C_2(w_c)$  is the linear  
 197 kinematic hardening. The symbol  $\langle \bullet \rangle$  corresponds to Macaulay's symbol such  
 198 that  $\langle x \rangle = 0$  if  $x < 0$  and  $\langle x \rangle = x$  if  $x \geq 0$ .

199 These two potentials automatically satisfy the second principle of thermo-  
 200 dynamics due to certain properties: non-negativity, convexity, and zero at the  
 201 origin ([33]).

202 As mentioned in section 2, the experimental tests are conducted when flax /  
 203 epoxy composite specimens reach mass equilibrium. Diffusion kinetics showed  
 204 that the moisture uptake of dried samples stored for 2 hours at laboratory  
 205 atmosphere condition is less than  $5 \cdot 10^{-2}$  % and no difference in tensile behaviour  
 206 between these two groups of samples was found. Hence moisture content is  
 207 considered constant during tests. Under these assumptions, the state laws are  
 208 written as in equations (eq. 10 and 11) and the evolution equations are written  
 209 in equations (eq. 12 to 14).

$$\sigma = E(w_c) \cdot \varepsilon_e \quad (10)$$

$$X_i = C_i(w_c) \alpha_i \quad (11)$$

$$\dot{\varepsilon}_{ve} + \dot{\varepsilon}_{vp} = \frac{1}{\eta(w_c)} (\sigma - X_1) + \frac{\langle f \rangle}{K(w_c)} \text{sign}(\sigma - X_2) \quad (12)$$

$$\dot{\alpha}_1 = \frac{1}{\eta(w_c)} (\sigma - X_1) \quad (13)$$

$$\dot{\alpha}_2 = \frac{\langle f \rangle}{K(w_c)} \text{sign}(\sigma - X_2) \quad (14)$$

210 The proposed model describes the elastic contribution with a linear spring  
 211  $E(w_c)$ . For the viscoelastic contribution, a classical Kelvin–Voigt model con-  
 212 stituted of a linear viscous damper  $\eta(w_c)$  and a linear spring  $C_1(w_c)$  – with  
 213 internal stress  $X_1$  – connected in parallel is chosen. As for the viscoplastic con-  
 214 tribution, a viscous damper  $K(w_c)$  and a linear spring  $C_2(w_c)$  – with internal  
 215 stress  $X_2$  – are required. A kinematic hardening in which the evolution of the  
 216 kinematic variable  $X_2$  is collinear with the evolution of the plastic strain is used.  
 217 The proposed model is a 6-parameter model ( $E(w_c)$ ,  $\eta(w_c)$ ,  $C_1(w_c)$ ,  $K(w_c)$ ,  
 218  $C_2(w_c)$  and  $\sigma_y(w_c)$ ). All these parameters are assumed to be a function of  
 219 water content. Abida et al. [19] showed that the evolutions of properties of flax  
 220 fabric reinforcement are non-linear in regard to water content. That’s why, in  
 221 the first approach proposed in this study, all the parameters are assumed to be  
 222 function of water content as in equation (eq. 15). **This hypothesis does not**  
 223 **limit the proposed strategy.**

$$h(w_c) = \xi \cdot (w_c + \delta)^n \quad (15)$$

224 The model constitutive equations (from eq. 7 to 14) are solved using a  
 225 algorithm based on Runge-Kutta method implemented into MATLAB® ([35]).  
 226 The table (tab. 2) summarizes the model parameters and the coefficients that  
 227 need to be identified in order to describe the material behaviour. The consti-  
 228 tutive material parameters are identified using an inverse method presented in  
 229 the next section.

Table 2: model parameters and coefficients to identify

Symbol	Model parameters	Coefficients to identify
$E(w_c)$ [MPa]	Young Modulus	$\xi_1, \delta_1, n_1$
$\eta(w_c)$ [MPa · s]	Viscosity coefficient in viscoelastic domain	$\xi_2, \delta_2, n_2$
$C_1(w_c)$ [MPa]	Viscoelastic stiffness	$\xi_3, \delta_3, n_3$
$K(w_c)$ [MPa · s]	Viscosity coefficient in viscoplastic domain	$\xi_4, \delta_4, n_4$
$C_2(w_c)$ [MPa]	Kinematic hardening coefficient	$\xi_5, \delta_5, n_5$
$\sigma_y(w_c)$ [MPa]	Initial yield stress	$\xi_6, \delta_6, n_6$

230 *4.2. Inverse method*

231 The constitutive model parameters are identified via the experimental mea-  
 232 surements using an inverse method approach. This approach consists in an  
 233 optimisation problem where the objective is to minimise the gap between the  
 234 experimental results and the model predictions. The database is composed of 2  
 235 creep tests and 1 relaxation test for each water content (18 tests in total). These  
 236 tests are chosen to allow a more accurate identification of the parameters. The  
 237 remaining relaxation tests are used to verify the validity of the modelling. This  
 238 approach requires a cost function. This latter is defined using a least squares  
 239 method and it is calculated from the experimental data and the model prediction  
 240 according to the equation (eq. 16).

$$g(\Theta) = \sum_{k=1}^{N_m} \left[ \sum_{i=1}^{N_k} \frac{(\Gamma_c(\Theta, t_i) - \Gamma_m(t_i))^2}{(\Gamma_{max}^k)^2 \cdot N_k} \right] \quad (16)$$

241 where:

- 242 •  $\Theta$  a vector that contains the unknown parameters to be identified. This  
 243 vector collects all the coefficients  $\xi_i, \delta_i$  et  $n_i$  required to give the relation  
 244 between the model parameters and water content (see table 2);
- 245 •  $N_m$  the number of tests in database used;
- 246 •  $N_k$  the number of records of the test number  $k$ ;

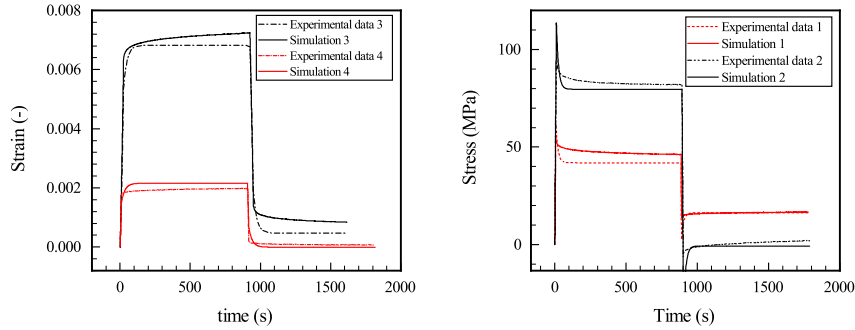
247 •  $\Gamma$  is the mechanical value into consideration for the test  $k$ . The subscripts  
 248  $m$  and  $c$  allow to distinguish the measured and the computed values re-  
 249 spectively.  $\Gamma_{max}^k$  is therefore the maximal value measured during the test  
 250  $k$ .  $\Gamma_{max}^k$  is a weighting and normalization coefficient. The proposed cost  
 251 function is therefore adimensional. The experimental data used in inverse  
 252 approach is composed of creep tests where  $\Gamma$  is the strain and relaxation  
 253 tests where  $\Gamma$  is the stress.

254 The identification is carried out using algorithms available on MATLAB® and  
 255 based on so-called simplex algorithms. These methods require an initial set  
 256 of parameters. In order to obtain a relevant one, the optimization problem is  
 257 decomposed into two stages. An auxiliary problem is firstly considered. Hence,  
 258 optimised material parameters for dried samples are firstly identified. This set of  
 259 parameters is used, in a second step, as initial parameters to obtain the material  
 260 parameters for the entire database (all water contents). In order to ensure the  
 261 stability and convergence of algorithms, several attempts are carried out using  
 262 different starting points. The evolution of Young modulus in function of water  
 263 content is directly extracted from experimental measurement to facilitate the  
 264 convergence of the algorithm, which means that the coefficients  $\xi_1$ ,  $\delta_1$  and  $n_1$   
 265 do not need to be identified.

## 266 5. Results and discussion

267 The intermediate identification stage consists in an inverse problem to iden-  
 268 tify the model coefficients (tab. 2) using only experiments conducted on dried  
 269 UD flax / epoxy laminates ( $w_c = 0\%$ ). In this case, the model is reduced  
 270 to a 6-parameter model where the coefficients ( $\xi_1$ ,  $\delta_1$ ,  $n_1$ ) are directly linked  
 271 to the material parameters (Young's modulus for instance). The correlation  
 272 between experimental data and simulation is good. The creep and relaxation  
 273 behaviour of UD flax / epoxy laminates is correctly predicted by the proposed  
 274 model (fig. 3a and 3b for creep and relaxation tests respectively). The stability  
 275 of algorithm convergence is checked by several attempts which consist of using

276 several starting points and perturbations in all parameters. No significant dif-  
 277 ference in the set of optimised parameters is found. Thus, the set of parameters  
 278 obtained by the optimisation procedure on dried UD flax / epoxy laminates is  
 279 relevant as a starting set and can be used for the inverse analyses on entire  
 280 experimental data taking into account all the water contents.



(a) creep tests at 50 MPa and 150 MPa (b) relaxation tests at 0.2 % and 0.35 %

Figure 3: intermediate stage optimisation results on dried composite

281 The inverse method approach defined in section 4.2 is used to extract con-  
 282 stitutive parameters of UD flax / epoxy laminates from 2 stress-level creep tests  
 283 and 1 relaxation test per water content (18 tests in total). Identification results  
 284 are given in (tab. 3).

285 The creep tests are conducted at two stress levels; one is below apparent  
 286 yield stress  $\sigma_c < R_e$  and the other is at 75 % of the ultimate stress (measured  
 287 via tensile tests)  $\sigma_c = 0.75 \cdot \sigma_u$ . The results show a pretty good agreement be-  
 288 tween model predictions and experimental data whatever the loading conditions  
 289 (fig. 4 and 5 for creep and relaxation tests respectively). As shown in figure (fig.  
 290 4), the strain evolution during creep and recovery stages as well as the perma-  
 291 nent strain after recovery at zero stress are satisfactorily predicted by the model  
 292 for both stress levels for water contents below 4.90 %. The stress relaxation and  
 293 antirelaxation phenomena (evolution of stress during unload) for these water  
 294 contents are also well described by the proposed model (fig. 5). However, for

Table 3: values of the model parameters and the identified coefficients

$\sigma_y(w_c)$ (MPa)	$\xi_2$	2.09	$\eta(w_c)$ (MPa · s)	$\xi_5$	202844
	$\delta_2$	0.25		$\delta_5$	0.04
	$n_2$	-2.13		$n_5$	-2.35
$K(w_c)$ (MPa · s)	$\xi_3$	2184	$C_1(w_c)$ (MPa)	$\xi_6$	3173
	$\delta_3$	0.15		$\delta_6$	0.29
	$n_3$	-3.45		$n_6$	-2.17
$C_2(w_c)$ (MPa)	$\xi_4$	2462			
	$\delta_4$	0.26			
	$n_4$	-2.28			

295 flax / epoxy composites at high water contents ( $w_c \geq 4.90\%$ ), model predictions  
 296 for creep and relaxation tests are satisfactory for those conducted at low stress  
 297 or strain (typically below apparent yield point). For high loading levels, the  
 298 evolution of the predicted stress and strain deviates from the measured ones as  
 299 shown in figures (fig. 4 and 5).

300 The model parameters are validated by comparing model predictions with  
 301 the relaxation tests that were not used for the identification procedure. The  
 302 validation is carried out using one test by water content. The results are plotted  
 303 in the figure (fig. 6). The same tendencies observed for identification tests are  
 304 perceived for validation ones. Indeed, a good agreement is observed for low  
 305 and medium water contents  $w_c < 4.90\%$  whatever the loading. However, a  
 306 discrepancy is noted between the predicted and the measured stresses for high  
 307 water contents.

308 This difference could be explained by the behaviour of these composites  
 309 at high water contents. Indeed, the tensile curves (fig. 1) show an apparent  
 310 rigidity increase from a certain level of deformation for high water contents  
 311 ( $w_c \geq 4.90\%$ ).

312 In order to confirm this assumption, simulation of monotonic tensile tests  
 313 are compared to experimental ones (fig. 7). As clearly visible, the tensile

314 behaviour until failure at water content below 4.90% is correctly predicted by  
315 the present model. For higher water contents, the apparent yield point is still  
316 adequately predicted and the tensile behaviour until the apparent rigidification  
317 point is still correctly described. However, the model predictions diverges from  
318 experimental data once rigidification phenomenon starts to appear (fig. 7). The  
319 figures (fig. 4 to fig. 7) confirm that the proposed model is able to describe the  
320 time-dependent behaviour and the hygromechanical coupling in flax / epoxy  
321 composites. The physical description of the model needs to be enhanced to  
322 include the rigidification mechanisms.

323 The initial yield stresses as a function of water content is extracted from  
324 experimental results and compared to the identified ones (figure 8). The exper-  
325 imental evolution of yield stress confirms the use of a power law to modelize  
326 the evolution of parameters in regards to water content. Nevertheless, for high  
327 water contents the yield stress is overestimated by the model and the onset of  
328 plasticity is delayed leading to an underestimation of the permanent strains in  
329 creep tests as already mentionned and shown in figure 4.

330 Besides, in this model, the viscoelastic and the viscoplastic phenomena are  
331 described by a unique characteristic time ( $\propto \eta$  and  $\propto K$  respectively). Hence,  
332 this apparent rigidity increase cannot be described by this model and the elastic  
333 contribution is underestimated which explains the tendencies observed in figures  
334 (fig. 4 and 5).

335 The evolutions of the viscoelastic and viscoplastic properties are plotted on  
336 figure (fig. 9). Viscosity in the viscoelastic ( $\eta$ ) and viscoplastic ( $K$ ) domains  
337 decreases with the water content (fig. 9a). It is also noted that the value of the  
338 parameter  $K$  is lower than the value of parameter  $\eta$  ( $K < 10^{-2}\eta$ ) regardless  
339 the water content. This indicates that viscoplastic phenomena are about 100  
340 times faster than viscoelastic ones. The decrease of both parameters points  
341 out that the viscoplastic and the viscoelastic phenomena are faster when water  
342 content increases. In addition, rigidity in the viscoelastic domain ( $C_1$ ) and in the  
343 viscoplastic domain ( $C_2$ ) also decreases with increasing water content (fig. 9b).  
344 Hence, the contribution of inelastic phenomena (viscoelastic and viscoplastic)

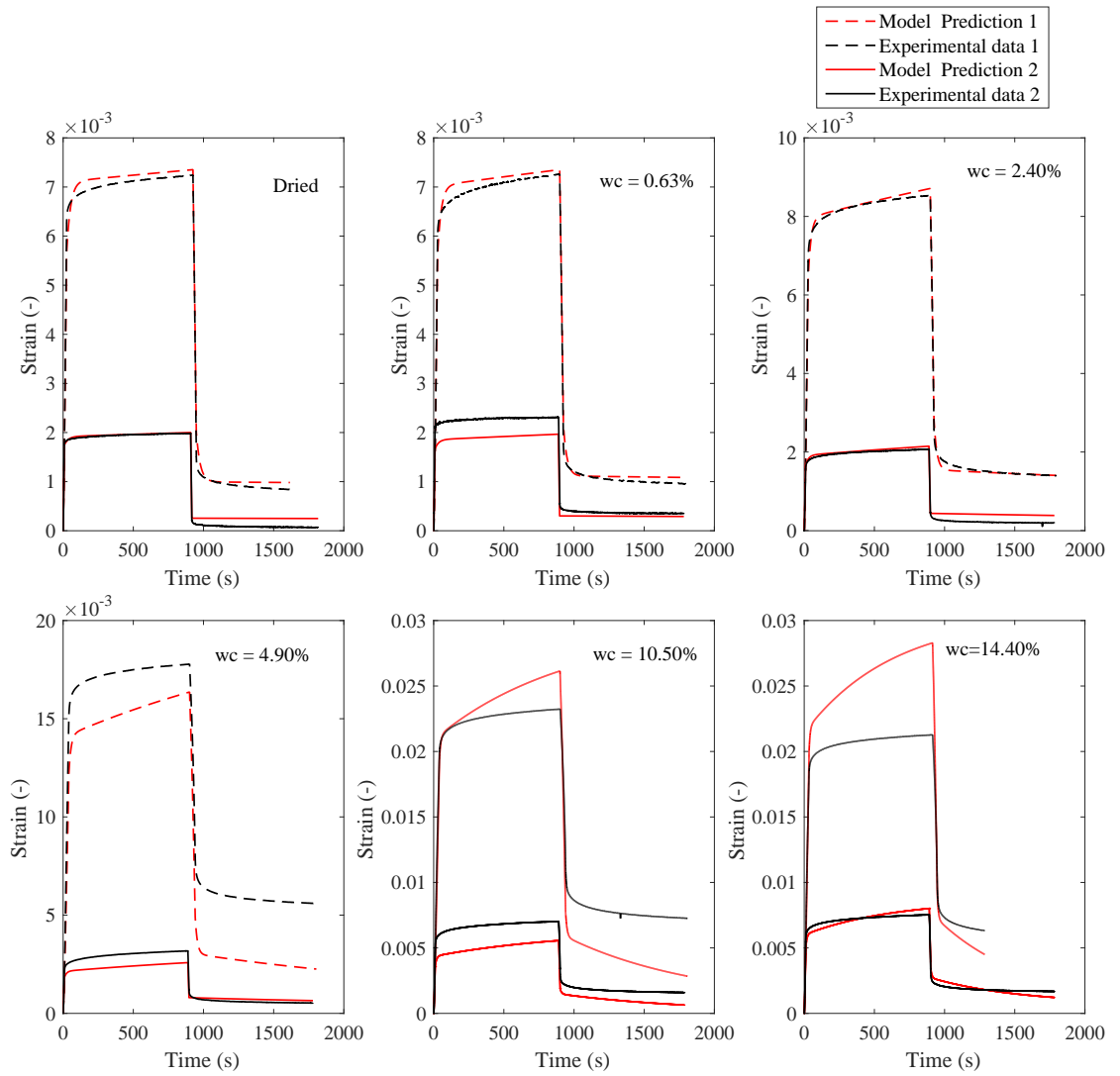


Figure 4: model prediction versus experimental data for creep tests at different water content

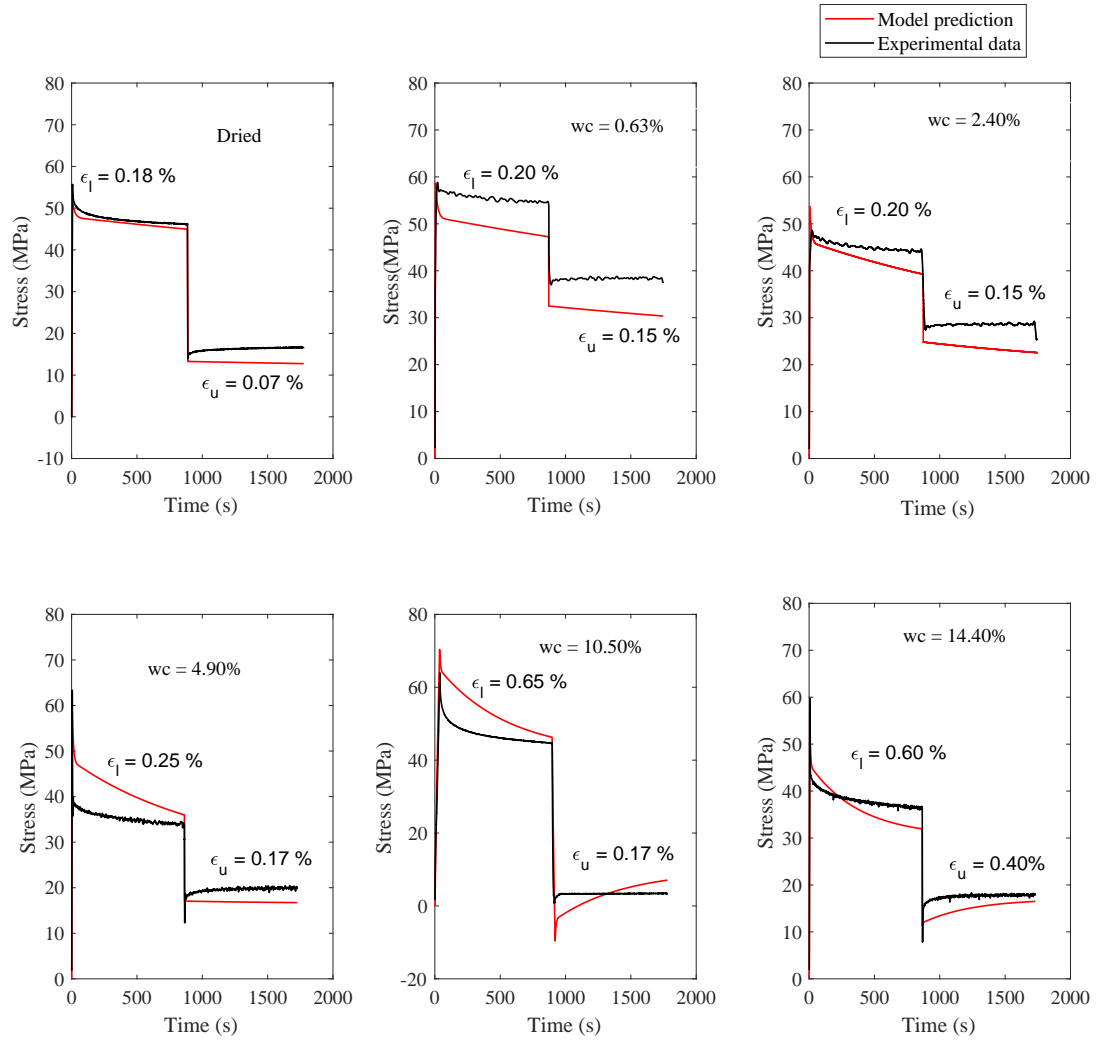


Figure 5: model prediction versus experimental data for relaxation tests at different moisture contents ( $\epsilon_l$  is the initial strain level and  $\epsilon_u$  is the strain after unloading)

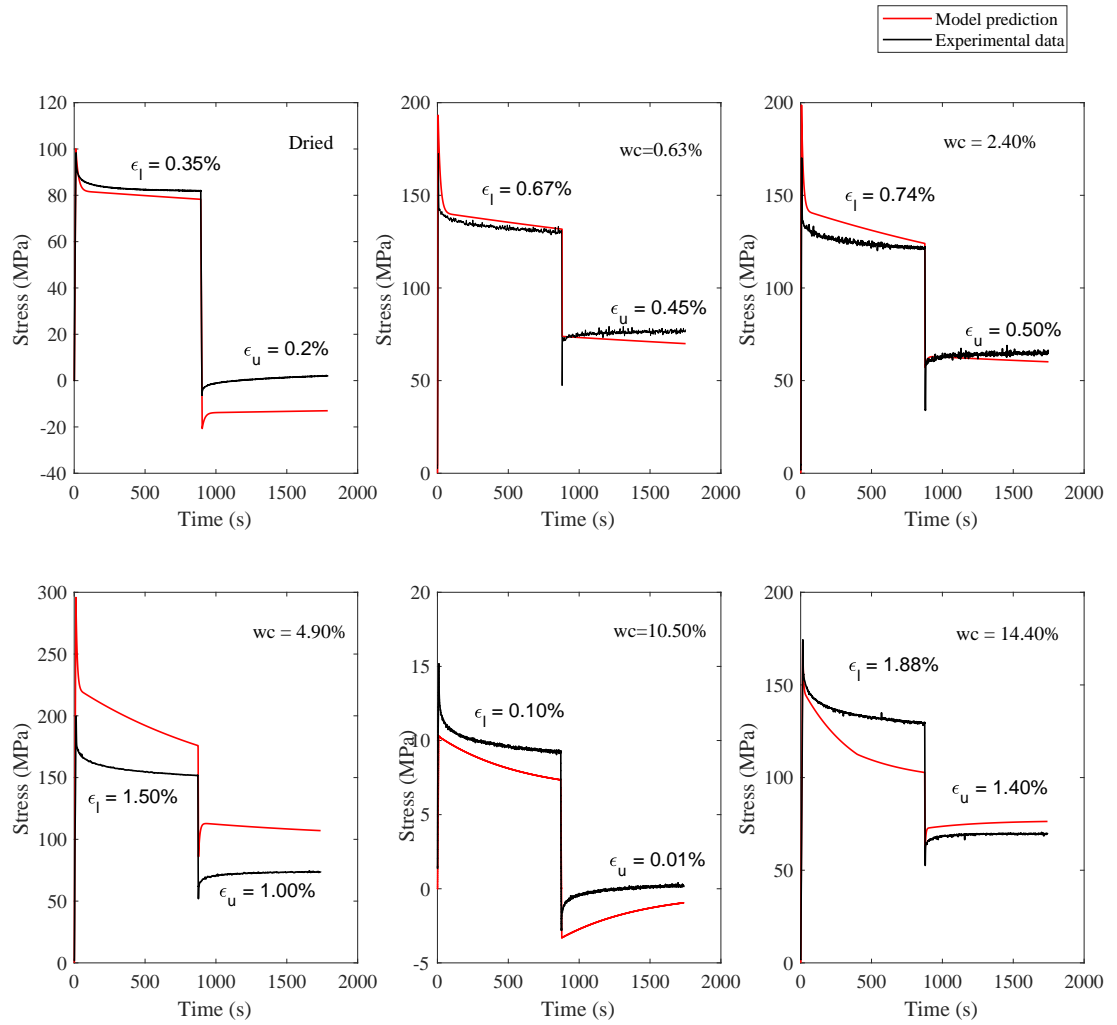


Figure 6: model validation on relaxation tests at different moisture contents ( $\epsilon_l$  is the initial strain level and  $\epsilon_u$  is the strain after unloading)

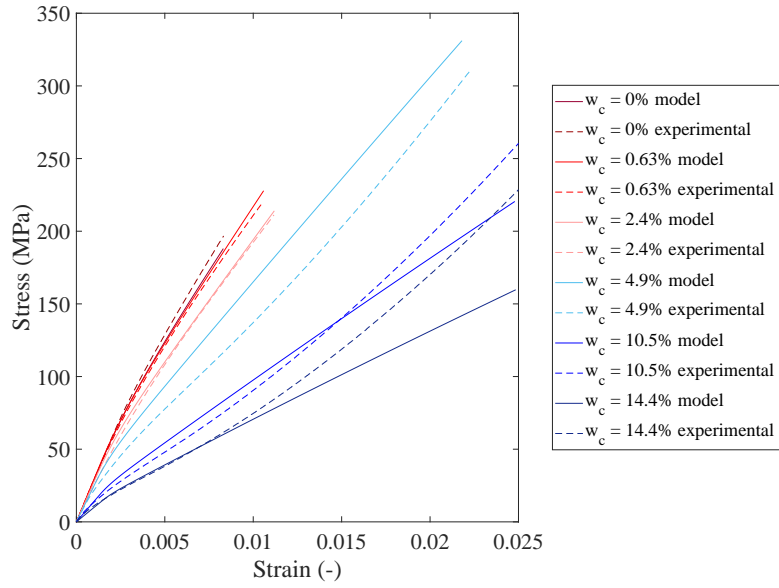


Figure 7: model validation with tensile tests

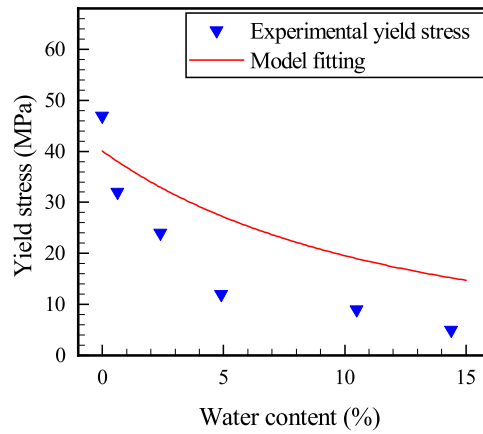
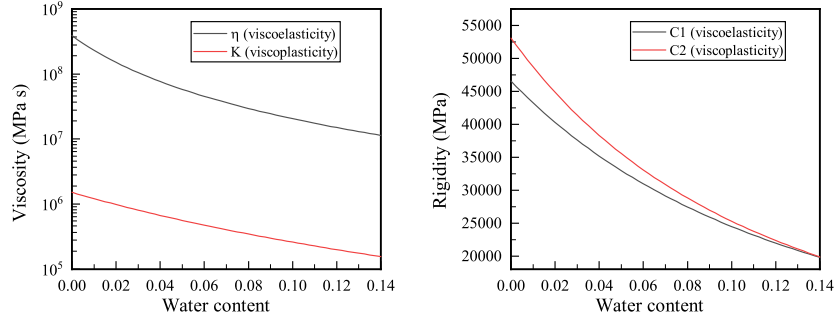


Figure 8: Comparison between experimental yield stress with model prediction

345 increases with the increase of water content.



(a) viscosity coefficient in viscoelastic and viscoplastic domains (b) rigidity in the viscoelastic and viscoplastic domains

Figure 9: evolution of viscoelastic and viscoplastic properties as a function of water content

## 346 6. Conclusion

347 The experimental investigation points out that the behaviour of flax rein-  
 348 forced epoxy composites is viscoelastic-viscoplastic with a strong hygromechan-  
 349 ical coupling. Based on this observation, a viscoelastic-viscoplastic model with  
 350 hygromechanical coupling is proposed in accordance with the general formal-  
 351 ism of small deformations and unidirectional loadings. From a rheological point  
 352 of view, the proposed model is a combination of a linear spring (elasticity),  
 353 a Kelvin-Voigt model (viscoelasticity) and a viscoplastic model described by  
 354 kinematic hardening in which the evolution of the internal variables is collinear  
 355 with the plastic deformation. It is therefore a 6-parameter model : the Young  
 356 modulus  $E(w_c)$ , the initial yield stress  $\sigma_y(w_c)$ , the viscosity coefficients in the  
 357 elastic and plastic domain  $\eta(w_c)$  and  $K(w_c)$  respectively, the viscoelastic stiff-  
 358 ness  $C_1(w_c)$  and the linear kinematic hardening  $C_2(w_c)$ . The hygromechanical  
 359 coupling is obtained via the dependence of all the model parameters to moisture  
 360 content according to a power law.

361 The constitutive parameters were extracted from experimental measure-  
362 ments using an inverse method approach. The proposed procedure leads to  
363 identify reliable model parameters. In the following, a highlight of the main  
364 conclusions is done:

- 365 • The time-dependent behaviour of flax / epoxy composites at low and mod-  
366 erate moisture contents ( $w_c < 4.90\%$ ) is correctly described by this model.  
367 The composite behaviour at high water contents ( $w_c \geq 4.90\%$ ) is also  
368 correctly described for loadings below the apparent stiffening point. How-  
369 ever, the model fails to predict the behaviour for high moisture contents  
370 ( $w_c \geq 4.90\%$ ) at loadings beyond the rigidification point.
- 371 • On the one hand, this model deviation was attributed to the emergence  
372 of a stiffening phenomenon at high water contents as observed in tensile  
373 tests. On the other hand, this discrepancy experiment/model could also  
374 be due to the initiation of plasticity which is not well identified.
- 375 • The analysis of modelling results also revealed an increase in non-elastic  
376 deformations (viscoelastic and viscoplastic) of flax / epoxy composites  
377 with increasing water content. The study shows a decrease in the viscos-  
378 ity parameters ( $\eta(w_t)$  and  $K(w_t)$ ) accompanied with a decrease in the  
379 associated rigidities ( $C_1(w_t)$  and  $C_2(w_t)$ ) with increasing water content.

### 380 **Declaration of conflicting interests**

381 The authors declare no potential conflicts of interest with respect to the  
382 research, authorship, and/or publication of this article.

### 383 **Funding**

384 This research received no specific grant from any funding agency in the  
385 public, commercial, or not-for-profit sectors.

386 **References**

- 387 [1] G. Lebrun, A. Couture, L. Laperrière, Tensile and impregnation behavior of  
388 unidirectional hemp / paper / epoxy and flax / paper / epoxy composites,  
389 Composite Structures 103 (2013) 151–160. doi:10.1016/j.compstruct.  
390 2013.04.028.
- 391 [2] A. Rubio-López, T. Hoang, C. Santiuste, Constitutive model to predict  
392 the viscoplastic behaviour of natural fibres based composites, Composite  
393 Structures 155 (2016) 8–18.
- 394 [3] K. Oksman, High Quality Flax Fibre Composites Manufactured by the  
395 Resin Transfer Moulding Process, Journal of reinforced plastics and com-  
396 posites 20 (2001) 621–627.
- 397 [4] M. Hughes, Æ. J. Carpenter, C. Hill, Deformation and fracture behaviour  
398 of flax fibre reinforced thermosetting polymer matrix composites, Journal  
399 of Material Science 42 (2007) 2499–2511.
- 400 [5] D. Scida, M. Assarar, C. Poilâne, R. Ayad, Influence of hygrothermal age-  
401 ing on the damage mechanisms of flax-fibre reinforced epoxy composite,  
402 Composites Part B: Engineering 48 (2013) 51–58.
- 403 [6] C. Poilâne, Z. E. Cherif, F. Richard, A. Vivet, B. Ben Doudou, J. Chen,  
404 Polymer reinforced by flax fibres as a viscoelastoplastic material, Composite  
405 Structures 112 (1) (2014) 100–112.
- 406 [7] L. Yan, N. Chouw, K. Jayaraman, Flax fibre and its composites - A review,  
407 Composites Part B: Engineering 56 (August) (2014) 296–317.
- 408 [8] Z. E. Cherif, C. Poilâne, L. Momayez, J. Chen, Optimisation d'un pré-  
409 imprégné lin / époxy industriel Influence de l'orientation des fibres, Revue  
410 des Composites et des Matériaux Avancésdoi:10.3166/rcma.21.119-128.
- 411 [9] H. N. Dhakal, Z. Y. Zhang, M. O. Richardson, Effect of water absorption on  
412 the mechanical properties of hemp fibre reinforced unsaturated polyester  
413 composites, Composites Science and Technology 67 (7-8) (2007) 1674–1683.

- 414 [10] S. Christian, S. Billington, Moisture diffusion and its impact on uniaxial  
415 tensile response of biobased composites, *Composites Part B: Engineering*  
416 43 (5) (2012) 2303–2312. doi:10.1016/j.compositesb.2011.11.063.
- 417 [11] M. Assarar, D. Scida, A. El Mahi, C. Poilâne, R. Ayad, Influence of water  
418 ageing on mechanical properties and damage events of two reinforced com-  
419 posite materials: Flax-fibres and glass-fibres, *Materials and Design* 32 (2)  
420 (2011) 788–795.
- 421 [12] A. Le Duigou, A. Bourmaud, P. Davies, C. Baley, Long term immer-  
422 sion in natural seawater of Flax/PLA biocomposite, *Ocean Engineering*  
423 90 (November) (2014) 140–148.
- 424 [13] P. Mannberg, B. Nyström, L. Wallström, R. Joffe, Service life assessment  
425 and moisture influence on bio-based composites, *Journal of Materials Sci-  
426 ence* 49 (15) (2014) 5265–5270. doi:10.1007/s10853-014-8211-6.
- 427 [14] F. K. Sodoke, L. Toubal, L. Laperrière, Hygrothermal effects on fatigue  
428 behavior of quasi-isotropic flax/epoxy composites using principal compo-  
429 nent analysis, *Journal of Materials Science* 51 (24) (2016) 10793–10805.  
430 doi:10.1007/s10853-016-0291-z.
- 431 [15] A. P. Kumar, M. N. Mohamed, A comparative analysis on tensile strength  
432 of dry and moisture absorbed hybrid kenaf/glass polymer composites,  
433 *Journal of Industrial Textiles* 47 (8) (2018) 2050–2073. doi:10.1177/  
434 1528083717720203.
- 435 [16] A. Alhuthali, I. M. Low, Mechanical properties of cellulose fibre rein-  
436 forced vinyl-ester composites in wet conditions, *Journal of Materials Science*  
437 48 (18) (2013) 6331–6340. doi:10.1007/s10853-013-7432-4.
- 438 [17] K. M. Mannan, Z. Robbany, Rotation of a natural cellulosic fibre about its  
439 fibre axis due to absorption of moisture, *Polymer* 37 (20) (1996) 4639–4641.  
440 doi:10.1016/0032-3861(96)00265-0.

- 441 [18] V. Placet, O. Cissé, M. Lamine Boubakar, Influence of environmental rela-  
442 tive humidity on the tensile and rotational behaviour of hemp fibres, Jour-  
443 nal of Materials Science 47 (7) (2012) 3435–3446.
- 444 [19] M. Abida, F. Gehring, J. Mars, A. Vivet, F. Dammak, Effect of hy-  
445 groscopy on non-impregnated quasi-unidirectional flax reinforcement be-  
446 haviour, Industrial Crops & Products 128 (September 2018) (2019) 315–  
447 322. doi:10.1016/j.indcrop.2018.11.008.  
448 URL <https://doi.org/10.1016/j.indcrop.2018.11.008>
- 449 [20] E. Marklund, J. Eitzenberger, J. Varna, Nonlinear viscoelastic viscoplastic  
450 material model including stiffness degradation for hemp/lignin composites,  
451 Composites Science and Technology 68 (9) (2008) 2156–2162.
- 452 [21] E. Kontou, G. Spathis, P. Georgiopoulos, Modeling of nonlinear  
453 viscoelasticity-viscoplasticity of bio-based polymer composites, Poly-  
454 mer Degradation and Stability 110 (2014) 203–207. doi:10.1016/j.  
455 polymdegradstab.2014.09.001.
- 456 [22] J. Andersons, J. Modniks, E. Sparnīns, Modeling the nonlinear deformation  
457 of flax-fiber-reinforced polymer matrix laminates in active loading, Journal  
458 of Reinforced Plastics and Composites 34 (3) (2015) 248–256. doi:10.  
459 1177/0731684414568043.
- 460 [23] A. Chilali, W. Zouari, M. Assarar, H. Kebir, R. Ayad, Analysis of the  
461 mechanical behaviour of flax and glass fabrics-reinforced thermoplastic and  
462 thermoset resins, Journal of Reinforced Plastics and Composites 35 (16)  
463 (2016) 1217–1232. doi:10.1177/0731684416645203.
- 464 [24] F. Richard, C. Poilâne, H. Yang, F. Gehring, E. Renner, A viscoelasto-  
465 plastic stiffening model for plant fibre unidirectional reinforced composite  
466 behaviour under monotonic and cyclic tensile loading, Composites Science  
467 and Technology 167 (April) (2018) 396–403.

- 468 [25] R. Schapery, Nonlinear viscoelastic and viscoplastic constitutive equations  
469 based on thermodynamics, *Mechanics of Time-Dependent Materials* 1 (2)  
470 (1997) 209–240. doi:10.1023/A:1009767812821.
- 471 [26] L. Pupure, J. Varna, R. Joffe, Methodology for macro-modeling of bio-  
472 based composites with inelastic constituents, *Composites Science and Tech-*  
473 *nology* 163 (2018) 41 – 48.
- 474 [27] L. Zapas, J. Crissman, Creep and recovery behaviour of ultra-high  
475 molecular weight polyethylene in the region of small uniaxial deforma-  
476 tions, *Polymer* 25 (1) (1984) 57 – 62. doi:https://doi.org/10.1016/  
477 0032-3861(84)90267-2.
- 478 [28] M. Abida, J. Mars, F. Gehring, A. Vivet, F. Dammak, Anisotropic elastic-  
479 viscoplastic modelling of a quasi-unidirectional flax fibre-reinforced epoxy  
480 subjected to low-velocity impact, Springer International Publishing, Cham,  
481 2018, pp. 171–178.
- 482 [29] A. Le Duigou, J. Merotte, A. Bourmaud, P. Davies, K. Belhouli, C. Ba-  
483 ley, Hygroscopic expansion: A key point to describe natural fibre/polymer  
484 matrix interface bond strength, *Composites Science and Technology* 151  
485 (2017) 228–233.
- 486 [30] E. Bosco, R. Peerlings, M. Geers, Scale effects in the hydro-thermo-  
487 mechanical response of fibrous networks, *European Journal of Mechan-*  
488 *ics, A/Solids* 71 (November 2017) (2018) 113–121. doi:10.1016/j.  
489 *euromechsol.2018.03.013*.
- 490 [31] A. Chilali, M. Assarar, W. Zouari, H. Kebir, R. Ayad, Analysis of the  
491 hydro-mechanical behaviour of flax fibre-reinforced composites: assess-  
492 ment of hygroscopic expansion and its impact on internal stress, *Compos-*  
493 *ite Structures* 206 (April) (2018) 177–184. doi:10.1016/j.compstruct.  
494 2018.08.037.

- 495 [32] V. Placet, O. Cissé, M. Lamine Boubakar, Nonlinear tensile behaviour of  
496 elementary hemp fibres. Part I: Investigation of the possible origins using  
497 repeated progressive loading with in situ microscopic observations, Com-  
498 posites Part A: Applied Science and Manufacturing 56 (2014) 319–327.
- 499 [33] J. Lemaitre, J. L. Chaboche, Mechanics of solid materials, Cambridge:  
500 Cambridge University Press, 1994.
- 501 [34] B. Halphen, Q. Son Nguyen, Sur les matériaux standard généralisés, Jour-  
502 nal de Mécanique 14 (1975) 39–63.  
503 URL <https://hal.archives-ouvertes.fr/hal-00105514>
- 504 [35] L. F. Shampine, M. W. Reichelt, The MATLAB ODE Suite, SIAM Journal  
505 on Scientific Computing 18 (1) (1997) 1–22.